ADVANCED FUNCTIONAL MATERIALS
www.afm-journal.de

Directional, Silanized Plant-Based Sponge for Oil Collection

Jongbeom Kim, Jingyu Deng, Nam-Joon Cho, and Seung Min Han**

Porous materials are commonly employed to combat marine pollution by absorbing oil. However, the release of microplastics or nanoparticles from their synthetic components further exacerbates environmental concerns. In this study, a sustainable and reusable pollen sponge derived from eco-friendly pollen grains and fabricated using a directional freeze-drying method is introduced for the first time. These grains undergo a defatting process followed by a controlled hydrolysis process, transforming them into a pollen microgel made of sporopollenin, the primary constituent of a pollen grain's outer layer. The directional freeze-drying technique is used to fabricate porous structures with controlled orientation using the pollen microgel. The application of a chemical vapor deposition with dodecyltrimethoxysilane (DDTS) grants sponge hydrophobic properties, making it ideal for selective oil absorption. This modified pollen sponge boasts superior absorption capacities (15–59 times its weight) compared to most natural sponges. Additionally, its excellent durability and ability to recover up to 65% of deformation even after 60% strain compression are remarkable with the silanization process tripling the recoverability of pollen sponges. Remarkably, the silanized directional pollen sponge (SDPS) retains this resilience after 100 compression cycles. Therefore, the SDPS emerges as an eco-conscious solution for repeated and selective oil absorption tasks.

1. Introduction

The natural environment offers invaluable resources like sunlight, air, and minerals, among which plants have been crucial for human needs, including food and shelter.[1] Pollen, a small part of plants, is vital for plant reproduction and has received much interest for its unique qualities, being nutrient-rich and therapeutic, making it a choice ingredient in superfoods and medicine.[2–4] To ensure reproductive efficacy, plants generate an abundance of pollen grains and spores, equipping them with the ability to protect against the harsh conditions of nature.[5–7] Pollen consists of four layers: pollenkitt, exine, intine, and cytoplasmic content,[8] and the outer exine is constructed with biopolymers with excellent chemical and mechanical stability called "sporopollenin" that serves as the layer that protects the genetic materials inside for plant reproduction. Altering the physical and chemical properties of pollen grains through processing results in versatile material building blocks employed in various cutting-edge fields such as drug delivery,[9] tissue engineering, soft robotics,[7] biosensors,[10] actuators,[11] flexible electronics,[12] and environmental cleanup.[13] Inspired by the concept of cross-economy,[14] the utilization of pollen has emerged as a remarkable example of sustainable resource transformation.[15] To achieve sustainable development goals,[16] it is necessary to explore radically new functions that challenge the inherent characteristics of natural materials. Pollen, often considered a byproduct of the plant reproduction process, is now recognized for its unique potential as a high-value material.[15]

Pollen plays a vital role in protecting the genetic material of plants by acting as a protective casing due to its inert properties. This biological function of pollen in the protection of genetic materials can be used to protect the environment through sustainable processes. As one of the major environmental pollutants, oil spills can have severe environmental and economic consequences,[17] and cleanup technologies such as containment booms, skimmers, and sorbents have been commonly employed to remove oil from the water surface and shoreline. These conventional cleanup technologies make use of non-reusable materials that in turn cause another environmental pollution, and thus the development of reusable absorbent materials for selective oil absorption has been of recent interest.[18–23] The most popular materials used for reusable absorbents are synthetic polymers,[24–28] and carbon nanomaterials[29–32] due to their excellent elastic properties, but yet with their own limitations. Synthetic polymers carry the risk of partial degradation in harsh marine environments, leading to the release of microplastics that lead to marine pollution[33] while carbon nanomaterial-based alternatives raise concerns regarding the ecological impact on marine ecosystems by effects of nanosized particles on organisms.[34] Therefore, many studies are underway in trying to replace these materials with nontoxic natural material alternatives.[35–37] An oil absorbent made from pollen as a renewable material holds great promise in addressing another aspect of environmental pollution.

J. Kim, S. M. Han
Department of Materials Science and Engineering
Korea Advanced Institute of Science and Technology (KAIST)
291 Daehak-ro, Yuseong-gu, Daejeon 34141, Republic of Korea
E-mail: smhan01@kaist.ac.kr

J. Deng, N.-J. Cho
School of Materials Science and Engineering
Nanyang Technological University
50 Nanyang Avenue 639798, Singapore
E-mail: njcho@ntu.edu.sg

The ORCID identification number(s) for the author(s) of this article can be found under https://doi.org/10.1002/adfm.202313808

DOI: 10.1002/adfm.202313808

Sporopollenin, composed of random copolymers of fatty acids, phenylpropanoids, and phenolic compounds, is one of the most chemically and mechanically inert biopolymers, with different functional groups attached to it depending on the plant species.[38,39] These functional groups present on sporopollenin make its surface hydrophobic through functional group modification. Connecting long carbon backbones to the hydroxyl group of the pollen surface using a silanization reaction,[40,41] the hydrophobicity of the pollen surface can be increased to elevate the oil absorption ability of the pollen structure. The improvement in hydrophobicity enhances capillary action for oil absorption by decreasing the surface tension between the oil and pollen surface.

In this study, a new 3D porous scaffold consisting of pollen was developed using a directional freeze-drying method as an eco-friendly reusable oil-absorbent material. A thermal gradient in one direction is imposed during freeze-drying to fabricate a 3D porous structure that consists of walls made from pollen building blocks.[42] The 3D porous structure with aligned orientation allows for excellent recovery and resilience, and the vertically aligned pores with hydrophobic modified surfaces allow for the use of capillary effect to facilitate oil absorption from the sea surface. The resulting directionally aligned pollen 3D structure termed salinized directional pollen sponge (SDPS) was thus designed and used in this study as a new oil absorption material with significant enhancement in absorption capacity, resilience, and thus lifetime.

2. Results and Discussion

2.1. Morphology of Directional Freeze-Dried Pollen Sponges

A 3D porous sponge composed of pollen walls was fabricated using pollen microgel through a freeze-drying method, which can manufacture a 3D porous structure with the inverse structure of ice crystals. Pollen microgel is composed of a mixture of water and sunflower pollen exine particles made of sporopollenin. Sporopollenin possesses an exceptionally high Young's modulus, ranging from 9.5 to 16 GPa, surpassing that of other biopolymers.[43] Additionally, the abundant presence of hydroxyl and carboxyl groups on the surface, along with a spiky micro/nano hierarchical surface morphology, aids in the self-crosslinking formation of the structural walls by sunflower pollen grains.[7,44] Therefore, sunflower pollen can be chosen as a highly suitable building block for creating a robust 3D material. A schematic image of the fabrication process of pollen sponges is illustrated in **Figure 1**a. The side of the mold containing the pollen microgel is made of an insulating material, and only the bottom of the solution is cooled to generate a temperature gradient in the vertical direction. Ice crystals are generated along the direction of the temperature gradient through a sublimation process, and a directionally aligned pore structure can be obtained by a directional freeze-drying process. The photographs of directionally freeze-dried pollen sponges are shown in Figure S1 (Supporting Information). A directional pollen sponge (DPS) with a size of 1.5 cm × 1.5 cm × 1.5 cm was fabricated. The density of the pollen sponge was 28.7 mg cm^{-3}. To confirm the pore geometry of the DPS, the freeze-dried sponges with vertical and horizontal directionality were cut in the horizontal direction as indicated in Figure S2 (Supporting Information), and the SEM cross-section image is shown in Figure 1b,c. The vertically grown DPS had anisotropic pores created by the sublimation of columnar-shaped ice crystals with a high aspect ratio that are found in Figure 1b. The high aspect ratio and small radius of these pores also maximize the capillary action that is needed for liquid absorption of the entire sponge structure. The directional freeze-drying method can control the growth of ice crystals, leading to changes in the pore structures of DPS from vertical to horizontal, and the aligned parallel walls of DPS from the directional freeze-drying method are shown in Figure 1c.

Surface modification of the DPS for enhancing oil absorption was performed by attaching dodecyltrimethoxysilane (DDTS) molecules to the surface using chemical vapor deposition. The reaction rate of this thermal-dependent reaction increases as the temperature rises from 70 to 250 °C.[45] In the case of DPS, a silanization reaction occurred noticeably at temperatures exceeding 125 °C. The photographs of fabricated DPS and SDPS with different reaction temperatures are shown in Figure S3 (Supporting Information). After the silanization reaction, the pollen sponge changed color from light yellow to brown, and its volume decreased by 44% due to heat-induced shrinking. Cross-sectional SEM images of the SDPS in Figure 1d,e show ertical and horizontal pore alignment, respectively. The average pore sizes of DPS and SDPS were measured as the length of the minor axis from cross-sectional SEM images of vertical pore sponges (Figure 1b,d), and Figure S4 (Supporting Information) shows their pore size distributions from cross-sectional SEM images cut in perpendicular to pore alignment. As the volume of the sponge decreased by silanization, the average pore size also decreased from 48.1 to 11.6 μm. The capillary force is known to be governed by two parameters: surface tension and pore radius. Silanization reaction therefore can maximize the capillary force from changing these two parameters, as it reduced the radius of the pores and decreased surface tension with nonpolar liquids from attached carbon backbones for more effective absorption of SDPS.

2.2. Spectroscopy-Based Characterization of Silanization Reaction

The pollen sponge fabricated using the directional freeze-drying method had a suitable structure for absorbing liquids because of its high porosity and high aspect ratio of the pores. However, the hydrophilic surface of pollen grains, resulting from functional groups such as hydroxyl and carboxyl groups, hinders selective oil absorption of the fabricated structure in the oil–water mixture. Therefore, to promote selective oil absorption of the DPS, surface modification of the walls of the pores of DPS to increase its hydrophobicity was performed. Among various surface modification methods such as chemical treatment with hydrophobic coating[46] or modifying surface structure,[47] the silanization reaction, where the alkoxy group of alkoxy silane covalently bonds hydroxyl groups to form oxygen bridges between Si and organic molecules was determined to be most compatible to increase the hydrophobicity of the DPS. Sporopollenin possesses numerous hydroxyl and phenolic moieties in its chemical structure,[38] and these readily react with the three methoxy groups present in the DDTS molecules to attach long carbon backbones onto the pollen

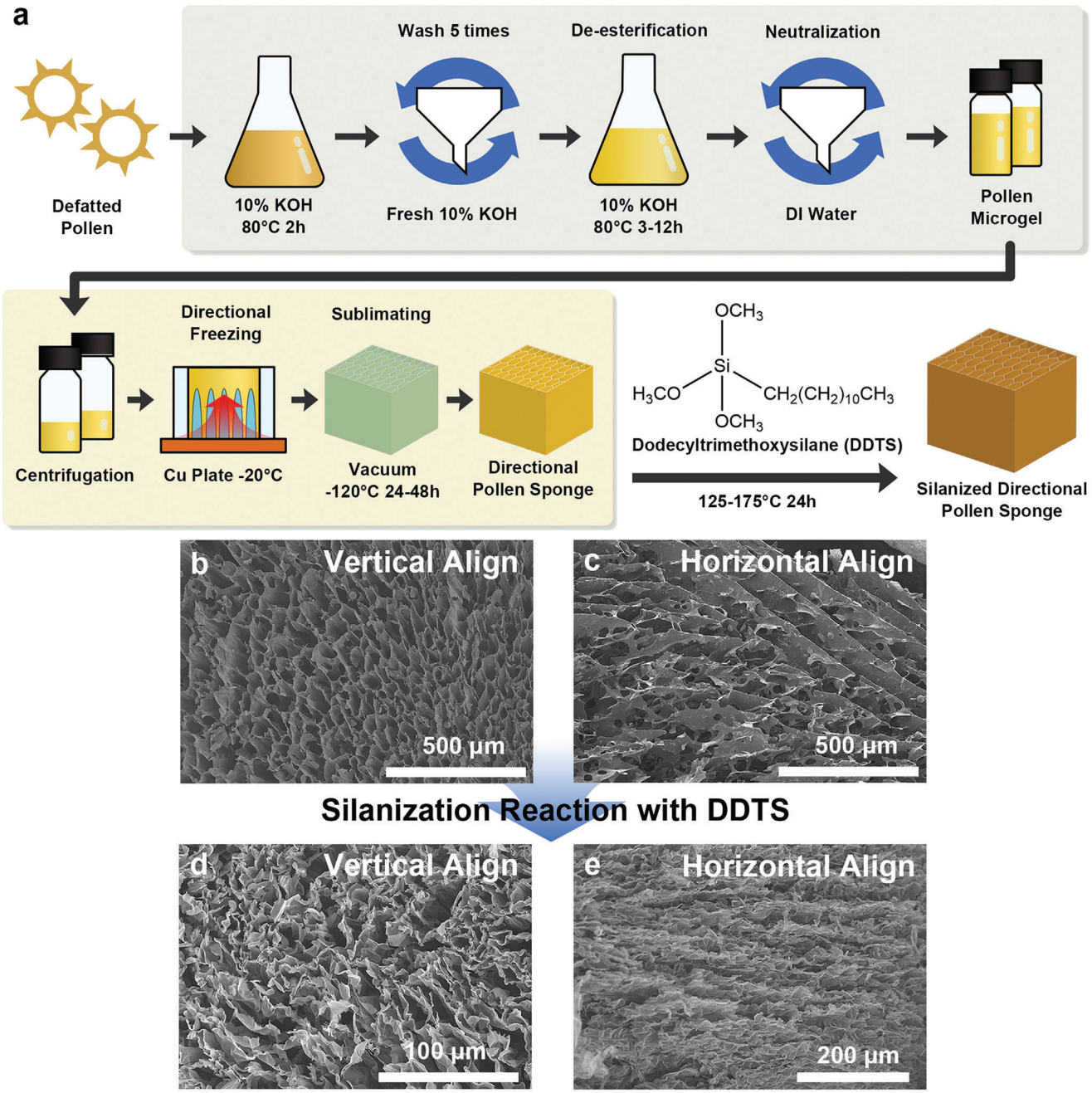

Figure 1. a) The schematic images of the SDPS fabrication process. SEM visuals of the DPS prepared by directional freeze-drying method, b) freeze-dried in a horizontal orientation, and c) freeze-dried in a vertical orientation. SEM visuals of the SDPS that was freeze-dried, d) horizontally, and e) vertically.

surface. As methoxy groups are more reactive than the ethoxy group and, unlike chlorosilane, do not produce hydrochloric acid as a byproduct, DDTS was selected for the silanization of the pollen sponge.

To verify the formation of oxygen bridges between pollen surfaces and DDTS, the binding state of the DPS, heat-treated DPS, and SDPS were analyzed by using FT-IR spectroscopy (**Figure 2**). Heat-treated DPS was included in order to distinguish peak changes caused by the silanization reaction from those resulting from heating. These three samples derived from the pollen microgel, where sporopollenin is the main component, exhibited similar patterns in the FT-IR spectra, and a detailed explanation is shown in Figure S5 (Supporting Information).

When these three FT-IR spectra were compared, two peaks were identified that significantly changed in the SDPS. The peak at 1051 cm^{-1} increased, while the peak at 1489 cm^{-1} disappeared. The absorption of Si—O—C vibration appears generally as a broad peak at 950–1250 cm^{-1}.[48] The broad peak at 1051 cm^{-1} could be assigned to the Si—O—C vibration in the SDPS. The peak at 1489 cm^{-1}, observed in the FT-IR spectra of the DPS,

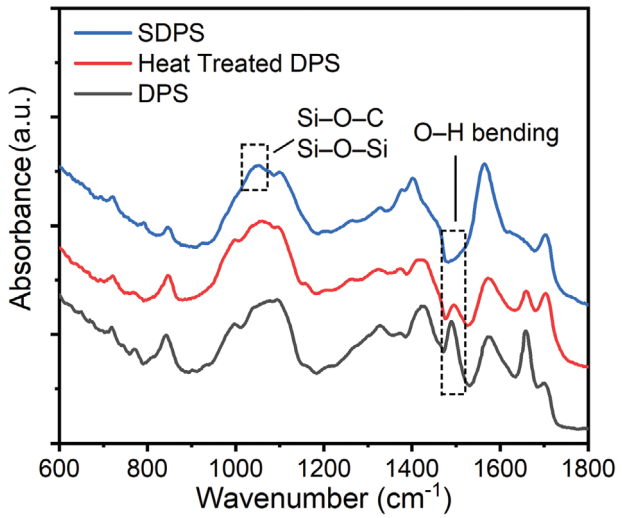

Figure 2. FT-IR spectra of the DPS, the heat-treated DPS, and SDPS.

corresponds to the O—H bending of the hydroxyl group attached to sporopollenin. As the silanization reaction proceeds, the hydroxyl group of the pollen and the methoxy group of DDTS react to form an oxygen bridge. Therefore, the content of hydroxyl groups in the DPS decreased sharply. In the spectra of the SDPS, the 1489 cm^{-1} peak corresponding to O—H bending disappeared. These changes in the FT-IR spectra indicate that the hydroxyl groups on the pollen surface no longer had the —OH form, but instead had the form of Si—O—C bridges. By comparing the spectra of the DPS with the SDPS, it was confirmed that DDTS successfully bound to the hydroxyl groups of the pollen by the silanization reaction.

The silanization reaction occurs more effectively as the temperature increases due to the influence of reaction kinetics, where higher temperature leads to increased mobility of silane molecules.[49,50] To investigate the thermal conditions of the silanization reaction, the Si peak of the SDPS was observed using XPS analysis while changing the reaction temperature. Each pollen sponge was fabricated using the same process mentioned above, and the silanization reaction was carried out by CVD at 125, 150, and 175 °C for 24 h. Conditions exceeding 200 °C were excluded from the experiment, as this resulted in extensive carbonization of the pollen sponge and severe deformation due to thermal shrinkage of its structure. The Si 2p peak graph for each temperature condition observed in the XPS analysis at 125, 150, and 175 °C is shown in **Figure 3**.

The Si 2p binding energy is sensitive to the atom attached to Si, allowing us to determine the ratio between carbon and oxygen bonded to the Si atom.[51] The Si in the DDTS molecule has Si—O—C bonds, observed at 102.2 ± 0.2 eV. This bond is associated with the methoxy group and the linkage between DDTS and pollen grains. The Si—C binding energy shown in the bond between the Si atom of DDTS and the carbon backbone is located at 101.3 ± 0.2 eV. For the silanized surface, the Si—O—Si binding energy is located at 103.2 ± 0.1 eV from the oxygen bridge formed between DDTS molecules. By calculating the relative peak area of each binding energy peak, we can infer how DDTS bound to the pollen sponge surface during the silanization reaction. The Si—O—C binding peak had an occupancy of 74–79%, showing that it was the main binding state of the Si atom in the SDPS. Evaluation of the XPS data shows that the proportion of the Si—C binding peak was the highest in the 175 °C sample. Specifically, this peak had the largest relative peak area in that sample, which indicates that the attachment of carbon backbones to the pollen surface was most efficient in the 175 °C sample. Therefore, the surface of the pollen sponge that was subjected to silanization at 175 °C had a higher density of carbon backbones than the surfaces of the pollen sponges that were reacted at lower temperatures. The reaction temperature of 175 °C, which produced pollen sponges with higher hydrophobicity, was therefore the most suitable for fabricating selective oil absorbents. Temperatures exceeding 200 °C, on the other hand, lead to significant carbonization of pollen sponges, making them unsuitable for reusable oil absorbers.

2.3. Reinforcement Effect of the Silanized Pollen Structure

Reliability in repeated compression is one of the most important performance factors in the development of reusable oil absorbents. The mechanical properties and reliability of pollen sponges were therefore obtained through a uniaxial cyclic compression test. Compression tests were performed in vertical and horizontal directions on freeze-dried pollen sponges with and without silanization and compression cycles were performed to 100 cycles. The pollen sponges used in the compression tests were prepared in cubes of 1 × 1 × 1 cm and the cyclic compression tests to the max strain of 60% were conducted at a relatively high strain rate of 1 min^{-1} to minimize strain-rate dependency of polymers.[52]

The results of the cyclic compression tests on the pollen sponges are presented in **Figure 4**. Figure 4a displays the stress-strain curves for the first cycle, while the other cycle data (5th, 10th, and 100th cycle) can be found in Figure S6 (Supporting Information). The stress–strain curves revealed that the vertically aligned structures exhibited greater strength, highlighting the anisotropic mechanical properties of the DPS as expected due to the directional alignment of the pores. The maximum recorded stress of DPS was 16.2 kPa for vertical alignment and 9.3 kPa for horizontal alignment. The vertically aligned structure had higher strength due to the honeycomb-like wall grown in the direction of loading while the horizontally aligned structure was observed to have lower strength due to less structural support from the walls. After silanization, the strength of the SDPS significantly increased regardless of the directional alignment; the maximum stress increased to 9.5 times from 16.2 to 154.7 kPa and 4 times from 9.3 to 35.4 kPa for vertical alignment and horizontal alignment, respectively. In comparison, the stress–strain curve for heat-treated vertically aligned DPS showed that heating increased the strength of the sponges to 1.4 times compared to sponges without heat treatment (Figure S7, Supporting Information), strongly suggesting that significant strength enhancement was achieved from the tethering of DDTS during the silanization process. In addition, the silanization reaction led to dehydration and shrinkage of the pollen sponges, which resulted in SDPS having a higher strength than DPS.

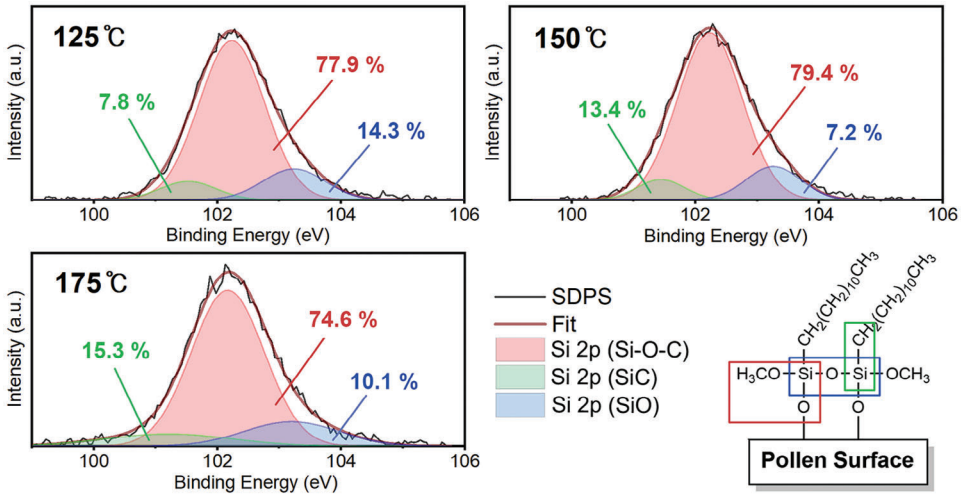

Figure 3. Si 2p XPS spectra of SDPS reacted at 125, 150, and 175 °C. The proportion of Si 2p(SiC) peak indicates how efficiently the carbon backbones are attached to the pollen sponge surfaces.

The high-temperature silanization process significantly enhanced the recoverability of pollen structures. The permanent strain was measured at the point where stress was completely relieved after one cycle of load-unload; the permanent strain decreased from 44.0% to 22.8% and from 43.7% to 21.2% in the vertical and horizontal alignment samples, respectively (Figure S6, Supporting Information). Figure 4b illustrates the changes in permanent strain during 100 cycles of compression for DPS and SDPS. DPS showed an increasing permanent strain closer to the maximum compressive strain. In contrast, even after 100 compression cycles, SDPS maintained a 43.9% permanent strain, demonstrating its ability to retain its shape during repeated compressions and suggesting its potential as a reusable oil absorbent. The horizontally aligned sponges exhibited a higher recoverability compared to the vertically aligned sponges. In the horizontal pore structures, the spaces between pores were compressed instead of the bending of the pollen walls. This prevented permanent deformation of the entire structures, resulting in a slight improvement in the recoverability of horizontal pollen sponges.

The SDPS exhibited higher strength and recoverability compared to the DPS in both pore directions. The mechanical strengthening of the pollen structure after silanization can be attributed to the enhanced connectivity between pollen grains. Pollen grains in the DPS formed their walls through hydrogen bonding.[53] These bare pollen walls, which are connected by relatively weak forces, were susceptible to deformation caused by external forces, and thus the strength and the recoverability of the entire sponge were low. In contrast, the SDPS interconnected pollen grains with covalent bonding and improved the pollen grain resilience to deformation via the silanization reaction. This difference in bonding methods for wall formation affected the resistance to wall deformation and enabled SDPS to have high strength and recoverability. Pollen grains strongly connected through covalent bonding maintained high recoverability even under repetitive deformations.

2.4. Absorption Test for Selective Oil Collecting

The water contact angle was measured to determine the increased hydrophobicity after the silanization reaction (**Figure 5a**). The contact angle is determined by the surface tension between the liquid and the substrate, and it increases as the surface

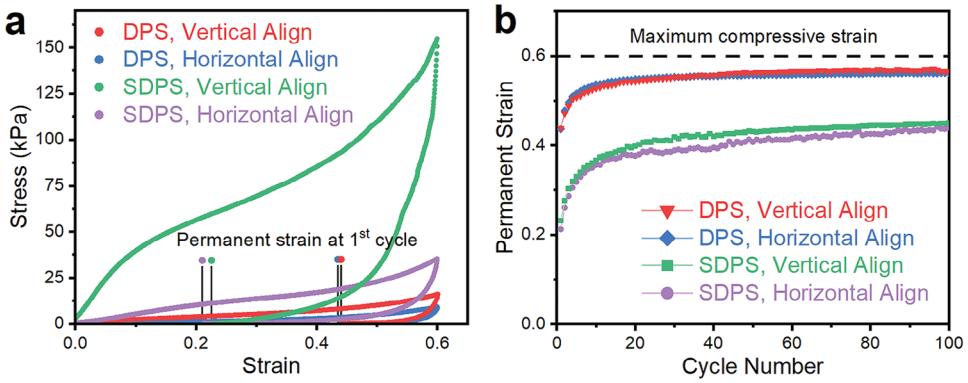

Figure 4. a) Results of first uniaxial compression test on DPS and SDPS with horizontal and vertical alignment indicating higher strain recoverability in SDPS. Permanent strain in each sample is marked for comparison. b) Permanent strain as a function of the compression cycle.

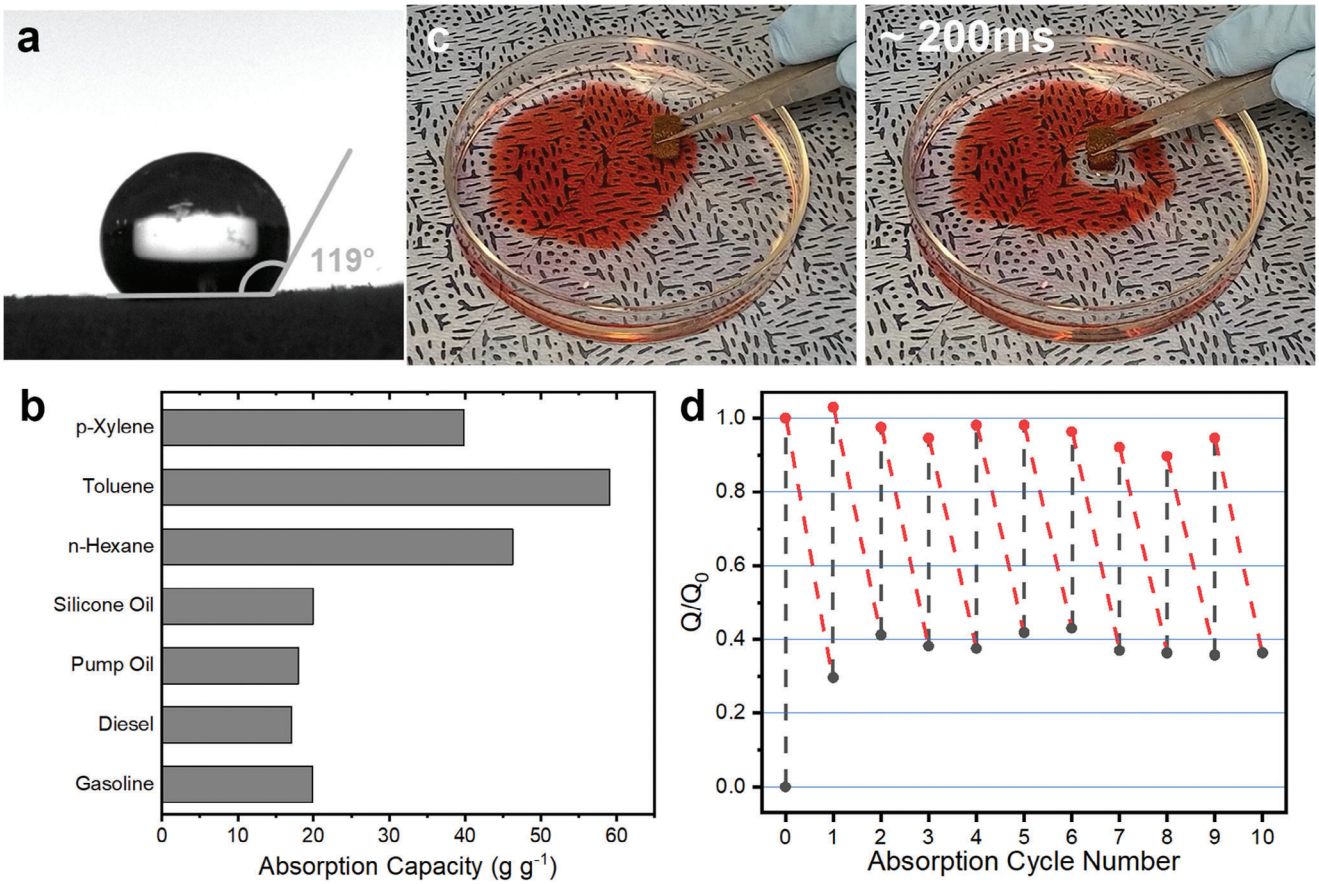

Figure 5. a) Contact angle test on the SDPS. b) Absorption capacity with various oils. c) Oil-O-Red stained *n*-hexane absorption test of the SDPS. d) Change of Q/Q_0 during the 10 cycles of squeezing after *n*-hexane absorption.

tension increases. Generally, a surface is defined as hydrophilic when the water contact angle is less than 90°, and conversely defined as hydrophobic if the angle exceeds 90°. The measured water contact angle on the SDPS surface was 119°, a significant increase in hydrophobicity relative to the water contact angle of DPS (Figure S8, Supporting Information). This phenomenon indicated that the pollen surface changed to a hydrophobic surface due to the attachment of carbon backbones through the silanization reaction.

To determine whether the SDPS produced in this study is suitable for use as an oil absorbent, experiments on absorption capacity were conducted. The absorption capacities of the SDPS were measured against various oils and chemical solvents. The liquids used in the absorption tests were commonly used nonpolar liquids and oils that are prone to leakage, including pump oil, diesel, gasoline, sunflower oil, *n*-hexane, *p*-xylene, toluene, and silicone oil. The absorption capacity was calculated by dividing the mass of the absorbed liquid by the initial mass of the absorbent. The absorption capacity is affected by the structure density, liquid density, and surface tension between the absorbing liquid and the pollen. The absorption capacity of the SDPS ranged from 15 to 59 times the mass of the sponge depending on the liquid used (Figure 5b). Demonstration of oil absorption was conducted using the fabricated SDPS, as shown in Figure 5c. The SDPS with vertically aligned pore quickly absorbed the surrounding *n*-hexane on the water surface as shown in Video S1 (Supporting Information). In the graph of recording absorption capacity of SDPS and random-oriented pore pollen sponge over time (Figure S9, Supporting Information), the oil absorption rate can be estimated based on the slopes of this graph. The slope of SDPS during the first 5 s was steeper than that of a random pore sponge, and the majority of absorption occurred within that initial 5 s period. However, the random pore structure indicates that complete absorption does not occur even after 60 s have elapsed. As it is known that pores aligned in a specific direction exhibit more effective absorption compared to randomly created pores,[54] the aligned pores of the SDPS, formed using the directional freeze-drying method, promoted more effective absorption than other oil absorbents primarily composed of randomly distributed pores.

The absorption capacity of the SDPS fabricated in this study was compared with that of other biopolymer absorbents (**Figure 6**). In particular, the absorption capacity increased by up to 30% depending on the type of liquid compared with a 3D pollen sponge composed of random pores.[55]

Cyclical oil recovery was studied to determine the reusability of the SDPS during oil absorption. 10 cycles of oil uptake and release by squeezing were performed and quantified to evaluate the oil recovery of SDPS. The absorption capacity of each absorption cycle was measured as Q, with the initial absorption capacity

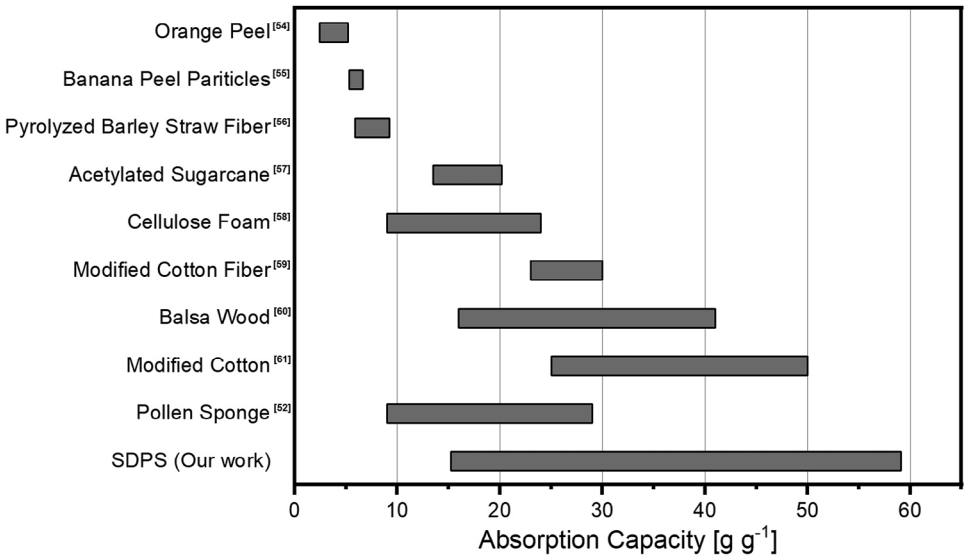

Figure 6. The absorption capacities of biomass absorbents[55–63] and SDPS show that SDPS has a higher oil absorption ability than other biomass absorbents.

denoted as Q_0, and the oil recovery was calculated as the difference between Q/Q_0 after squeezing. The graph of Q/Q_0 during the cyclic absorption test is shown in Figure 5d. During repeated absorption cycles, the average oil recovery after squeezing oil was maintained at 60%. This sustained oil recovery was achieved through the freeze-dried pore structure and structural reinforcement from silanization that was confirmed in mechanical testing. This indicated that the SDPS maintain their structures during the repeated oil absorption-squeezing process. Therefore, the SDPS demonstrates high potential as an eco-friendly, reusable, and selective oil absorbent.

3. Conclusion

In this study, eco-friendly anisotropic pore-structured silanized directional pollen sponges were manufactured using the directional freeze-drying method. The silanization reaction using CVD increased the hydrophobicity of the pollen sponges by shielding the hydrophilic hydroxyl groups on the pollen sponge surface with hydrophobic carbon backbones of DDTS, and the formation of oxygen bridges as a result of the silanization reaction was verified by FT-IR spectroscopy and XPS analysis. The increased hydrophobicity contributed to a decrease in interfacial tension between the SDPS surface and nonpolar liquids, and this in turn increased the capillary force for nonpolar liquids. The anisotropic pore structure of the sponges obtained using the directional freeze-drying method induced a greater capillary force due to smaller pore size and increased affinity with nonpolar liquids. The oxygen bridges generated by the silanization reaction improved the mechanical durability of the SDPS by replacing the hydrogen bonds between the pollen grains with covalent bonds. The recoverability of the SDPS increased by a maximum of 65% when mechanical deformation was exerted perpendicular to the aligned pore direction of the freeze-dried structure. These factors of increased capillary force and recoverability of SDPS demonstrate the potential of the fabricated sponge in repeatable oil absorption. SDPS exhibited a higher oil absorption capacity of 15.2–59.1 g g^{-1} compared with absorbents made from other natural materials. Taken together, SDPS was prepared and demonstrated its potential as an eco-friendly oil absorbent with high oil absorption ability and recovery.

4. Experimental Section

Sunflower Bee Pollen Defatting: Bee pollen (500 g) was combined with deionized (DI) water (1 L, 50 °C) and stirred for 2 h. The mixture was then strained through a 200-µm pore-sized nylon mesh to remove impurities such as sand. Vacuum filtration was used to collect the remaining pollen, which was then combined with 1 L of acetone at 25 °C. A disperser (IKA, Staufen, Germany) was used to stir the mixture at 800 rpm for 3 h before filtering. The pollen was washed 3–4 times with fresh acetone until the filtrate became clear. The pollen powder was then left in a fume hood for 12 h to evaporate any remaining acetone. Afterward, the dried pollen powder was mixed with diethyl ether (1 L) and stirred at room temperature for 2 h. This procedure was repeated two more times. The pollen was then combined with an additional 1 L of diethyl ether and stirred overnight to complete the reactions. Finally, the pollen powder was placed in a glass Petri dish and left in the fume hood to fully dry, resulting in the defatted pollen powder.

Microgel Preparation from Pollen: First, 20 g of defatted pollen was combined with a 10 wt% KOH aqueous solution (200 mL) and heated to 80 °C for 2 h while stirring at 800 rpm. Afterward, the mixture was filtered using a 35-µm pore-sized nylon mesh, and the collected pollen samples were rinsed with a fresh 10 wt% KOH solution until the filtrate appeared clear. The samples then underwent a de-esterification process that was incubated at 80 °C in a 10 wt% fresh KOH solution for 3–15 h, as detailed in the previous study.[64] To neutralize the samples, they were washed with DI water and filtered using the same 35-µm pore-sized nylon mesh until the pH value reached ≈7.5. This resulted in the formation of pollen microgels.

Fabrication of Freeze-Dried Directional Pollen Sponge: A pore-aligned pollen 3D porous structure was prepared from the pollen microgel above. The pollen microgel was centrifuged at 12 000 rpm for 1 h, and the supernatant liquid was removed. The resultant condensed microgel was collected in a vial in preparation for the freeze-drying process. The collected condensed microgel was pipetted into a square mold made of insulating

material on a copper plate. Controlled directional freezing was performed by cooling the bottom copper plate on dry ice with the acrylic plate as a thermal insulator to maintain a surface temperature of −20 °C. The frozen solution was lyophilized at −120 °C for 24–48 h to completely eliminate ice crystals from the entire structure using a freeze-dryer (FDCF-12006, Operon Co., South Korea).

Surface Modification of Pollen 3D Structures: The DPS surface property was modified using a one-step silanization reaction to imbue hydrophobicity to the prepared DPS. At high temperatures over 125 °C, DDTS (Sigma-Aldrich, St. Louis, MO), which has a long carbon backbone after the silicon atom, reacts with the hydroxyl groups of the pollen grains through chemical vapor deposition. The DPS was converted to the SDPS by enclosing one 1.5 cm × 1.5 cm × 1.5 cm DPS cube with 50 µL of DDTS in a sealed reaction vessel and heating at either 125, 150, or 175 °C for 24 h.

Functional Materials Characterizations: The surface and pore morphology of the pollen sponges were examined using SEM (SU5000, Hitachi, Japan). To analyze changes in the pollen surface after the silanization reaction, Fourier-transform infrared (FT-IR) spectroscopic analysis was conducted using a Nicolet iS50 FT-IR spectrometer (Thermo Fisher Scientific, Waltham, MA). The bare DPS, the heat-treated DPS, and the SDPS were used for FT-IR analysis for the comparison of the effect of silanization and heat treatment. To determine the optimal temperature for the silanization reaction of the pollen structure, X-ray photoelectron spectroscopic (XPS) analysis was performed with the SDPS using the K-Alpha XPS system (Thermo Fisher Scientific, Waltham, MA). The silanization temperature was set at 125, 150, and 175 °C, and then each SDPS was measured with the XPS system to semi-quantitatively analyze the Si (2p) peaks.

Uniaxial Cyclic Compression Testing: To identify changes in the mechanical behavior in repeated stimulation, cyclic compression tests were conducted on the DPS and SDPS using Insight 1 (MTS Instruments, Minneapolis, MN). The pollen sponges were held between two parallel plates and then uniaxial compressive stress was applied to the block-shaped pollen sponges. Each sample was tested with vertical and horizontal pore alignments. The compression strain rate was 1 min^{-1}, excluding the creep effect of polymeric materials by a fast testing speed. The tests were performed up to a strain of 60% for each sample and repeated 100 times to assess reliability during oil extraction. Careful alignment between the sample and the plate with a horizontally cut pollen structure is required to obtain a reliable loading curve.

Contact Angle Measurement: The contact angle between the SDPS surface and distilled water was measured to determine its hydrophobicity. Distilled water (0.05 mL) was dropped onto the flat surface of the vertical SDPS in the direction with pores, and then the angle was measured between the surface and the tangent line of the water drop outline at the three-phase contact point. The angle between the water drop tangent and the pollen surface was measured using the sessile drop method with a Phoenix 300 contact angle analyzer (South Korea, SEO Inc.).

Oil Absorption Measurements: The absorption capacity (Q) of the SDPS was calculated as follows:

$$Q \cdot \left(g \cdot g^{-1}\right) = \left(w - w_0\right) / w_0 \quad (1)$$

where w_0 is the mass of the SDPS, and w is the mass of the SDPS after oil absorption. The SDPS was immersed in oils and organic solvents (toluene, chloroform, dichloromethane, *n*-hexane, cyclohexane, silicone oil, pump oil, gasoline, diesel, and sunflower oil) for 5 min. The absorption capacity was measured for each solvent. To measure the recycling capabilities in the oil absorption process, absorption and squeezing cycles of *n*-hexane were performed 10 times, and the oil recovery (Q/Q_0) was measured in each cycle.

Supporting Information

Supporting Information is available from the Wiley Online Library or from the author.

Acknowledgements

This research was supported by the Creative Materials Discovery Program through the National Research Foundation of Korea (NRF) funded by the Ministry of Science and ICT(2020M3D1A1110524) and the National Research Foundation of Korea (NRF) funded by the Korean government (MSIT) under the grant NRF-2023R1A2C2004977. This work was also financially supported by the Tier 3 program (Grant No. MOET32022-0008) Ministry of Education Singapore. Aspire League Funding from joint project collaboration between KAIST, NTU, HSKUST, and TIT.

Conflict of Interest

The authors declare no conflict of interest.

Data Availability Statement

The data that support the findings of this study are available from the corresponding author upon reasonable request.

Keywords

directional freeze-drying, oil absorbents, pollen

Received: November 5, 2023
Revised: December 23, 2023
Published online:

[1] G. G. Marten, F. Taylor, *Human Ecology: Basic Concepts for Sustainable Development*, Routledge, an imprint of Taylor and Francis, Boca Raton, FL, **2010**.
[2] M. Filipiak, K. Kuszewska, M. Asselman, B. Denisow, E. Stawiarz, M. Woyciechowski, J. Weiner, *PLoS One* **2017**, *12*, 0183236.
[3] A. D. Vaudo, J. F. Tooker, C. M. Grozinger, H. M. Patch, *Curr. Opin. Insect Sci.* **2015**, *10*, 133.
[4] R. Moerman, M. Vanderplanck, D. Fournier, A. L. Jacquemart, D. Michez, *Insect Conserv. Diver.* **2017**, *10*, 171.
[5] E. Katifori, S. Alben, E. Cerda, D. R. Nelson, J. Dumais, *Proc. Natl. Acad. Sci.* **2010**, *107*, 7635.
[6] G. Mackenzie, A. N. Boa, A. Diego-Taboadal, S. L. Atkin, T. Sathyapalan, *Front. Mater.* **2015**, *2*, 55.
[7] Z. Zhao, Y. K. Hwang, Y. Yang, T. F. Fan, J. H. Song, S. Suresh, N. J. Cho, *Proc. Natl. Acad. Sci. U.S.A.* **2020**, *117*, 8711.
[8] J. Heslopharrison, Y. Heslopha, R. B. Knox, B. Howlett, *Ann Bot-London* **1973**, *37*, 403.
[9] R. C. Mundargi, M. G. Potroz, S. Park, H. Shirahama, J. H. Lee, J. Seo, N. J. Cho, *Small* **2016**, *12*, 1167.
[10] L. L. Wang, J. A. Jackman, W. B. Ng, N. J. Cho, *Adv. Funct. Mater.* **2016**, *26*, 8623.
[11] C. C. Mayorga-Martinez, M. Fojtu, J. Vyskocil, N. J. Cho, M. Pumera, *Adv. Funct. Mater.* **2022**, *32*, 2207272.
[12] L. L. Wang, J. A. Jackman, E. L. Tan, J. H. Park, M. G. Potroz, E. T. Hwang, N. J. Cho, *Nano Energy* **2017**, *36*, 38.
[13] T. Maric, M. Z. M. Nasir, N. F. Rosli, M. Budanovic, R. D. Webster, N. J. Cho, M. Pumera, *Adv. Funct. Mater.* **2020**, *30*, 2000112.
[14] N. J. Cho, *Mater. Today* **2022**, *61*, 1.
[15] T. Hornick, A. Richter, W. S. Harpole, M. Bastl, S. Bohlmann, A. Bonn, J. Bumberger, P. Dietrich, B. Gemeinholzer, R. Grote, B. Heinold, A. Keller, M. L. Luttkus, P. Mader, E. M. Svara, S. Passonneau, S. W. Punyasena, D. Rakosy, R. Richter, W. Sickel, I. Steffan-Dewenter, P. Theodorou, R. Treudler, B. Werchan, M. Werchan, R. Wolke, S. Dunker, *Plants People Planet* **2022**, *4*, 110.

[16] U. N. S. Commission, Global sustainable development report **2015**, https://sustainabledevelopment.un.org/content/documents/1758GSDR%202015%20Advance%20Unedited%20Version.pdf.
[17] C. Sheppard, *World Seas.: An Environmental Evaluation*, 2nd ed., Academic Press, London **2019**.
[18] Y. Liu, J. K. Ma, T. Wu, X. R. Wang, G. B. Huang, Y. Liu, H. X. Qiu, Y. Li, W. Wang, J. P. Gao, *ACS Appl. Mater. Interfaces* **2013**, *5*, 10018.
[19] L. Dashairya, M. Rout, P. Saha, *Adv. Compos. Hybrid Mater.* **2018**, *1*, 135.
[20] R. J. Lin, A. Li, T. T. Zheng, L. B. Lu, Y. Cao, *RSC Adv.* **2015**, *5*, 82027.
[21] A. M. Lazim, D. L. Musbah, C. C. Chin, I. Abdullah, M. H. A. Mustapa, A. Azfaralariff, *Polym. Test.* **2019**, *73*, 39.
[22] J. Zhao, Q. J. Guo, X. Wang, H. L. Xie, Y. Z. Chen, *Colloid Surface A* **2016**, *488*, 93.
[23] O. Oribayo, X. S. Feng, G. L. Rempel, Q. M. Pan, *Chem. Eng. J.* **2017**, *323*, 191.
[24] A. A. Nikkhah, H. Ziloueі, A. Asadinezhad, A. Keshavarz, *Chem. Eng. J.* **2015**, *262*, 278.
[25] A. M. Atta, W. Brostow, T. Datashvili, R. A. El-Ghazawy, H. E. H. Lobland, A. R. M. Hasan, J. M. Perez, *Polym. Int.* **2013**, *62*, 116.
[26] J. Zhao, C. F. Xiao, N. K. Xu, *Environ. Sci. Pollut. Res.* **2013**, *20*, 4137.
[27] S. K. Yeh, Y. B. Tsai, K. F. Gebremedhin, T. Y. Chien, R. Y. Chang, K. L. Tung, *Polym. Eng. Sci.* **2021**, *61*, 1139.
[28] Y. Y. Wang, X. H. Liu, M. Lian, G. Q. Zheng, K. Dai, Z. H. Guo, C. T. Liu, C. Y. Shen, *Appl. Mater. Today* **2017**, *9*, 77.
[29] H. Y. Mi, X. Jing, A. L. Politowicz, E. Chen, H. X. Huang, L. S. Turng, *Carbon* **2018**, *132*, 199.
[30] D. Kukkar, A. Rani, V. Kumar, S. A. Younis, M. Zhang, S. S. Lee, D. C. W. Tsang, K. H. Kim, *J. Colloid. Interf. Sci.* **2020**, *570*, 411.
[31] J. Y. Wu, A. K. An, J. X. Guo, E. J. Lee, M. U. Farid, S. Jeong, *Chem. Eng. J.* **2017**, *314*, 526.
[32] B. Wang, R. Karthikeyan, X. Y. Lu, J. Xuan, M. K. H. Leung, *Ind. Eng. Chem. Res.* **2013**, *52*, 18251.
[33] M. Bundschuh, J. Filser, S. Luderwald, M. S. Mckee, G. Metreveli, G. E. Schaumann, R. Schulz, S. Wagner, *Environ Sci Eur* **2018**, *30*, 1.
[34] A. B. Seabra, A. J. Paula, R. de Lima, O. L. Alves, N. Duran, *Chem. Res. Toxicol.* **2014**, *27*, 159.
[35] M. Ul-Islam, F. Subhan, S. U. Islam, S. Khan, N. Shah, S. Manan, M. W. Ullah, G. Yang, *Int. J. Biol. Macromol.* **2019**, *137*, 1050.
[36] L. Li, Z. Z. Xu, W. Sun, J. Chen, C. L. Dai, B. Yan, H. B. Zeng, *J. Membrane Sci.* **2020**, *598*, 117661.
[37] L. Y. Wang, Y. Y. Zhong, C. T. Qian, D. Z. Yang, J. Nie, G. P. Ma, *Acta Biomater.* **2020**, *114*, 193.
[38] F. S. Li, P. Phyo, J. Jacobowitz, M. Hong, J. K. Weng, *Nat Plants* **2019**, *5*, 41.
[39] R. Kesseler, M. M. Harley, *Pollen: The Hidden Sexuality of Flowers*, 1st ed., Papadakis Publisher, London, **2006**.
[40] J. B. Brzoska, I. Benazouz, F. Rondelez, *Langmuir* **1994**, *10*, 4367.
[41] X. Li, Y. Zhou, *Microfluidic Devices for Biomedical Applications*, 1st ed., Woodhead Publishing, Cambridge, UK, **2013**.
[42] L. Qian, H. F. Zhang, *J. Chem. Technol. Biot.* **2011**, *86*, 172.
[43] Z. H. Qu, J. C. Meredith, *J. R. Soc. Interface* **2018**, 15.
[44] T. F. Fan, S. Park, Q. Shi, X. Y. Zhang, Q. M. Liu, Y. Song, H. Chin, M. S. Bin Ibrahim, N. Mokrzecka, Y. Yang, H. Li, J. H. Song, S. Suresh, N. J. Cho, *Nat. Commun.* **2020**, *11*, 1449.
[45] B. Qiao, T. J. Wang, H. Gao, Y. Jin, *Appl. Surf. Sci.* **2015**, *351*, 646.
[46] C. R. Crick, I. P. Parkin, *Chemistry* **2010**, *16*, 3568.
[47] Z. Yoshimitsu, A. Nakajima, T. Watanabe, K. Hashimoto, *Langmuir* **2002**, *18*, 5818.
[48] C. A. Hacker, K. A. Anderson, L. J. Richter, C. A. Richter, *Langmuir* **2005**, *21*, 882.
[49] J. M. Jin, J. W. M. Noordermeer, W. K. Dierkes, A. Blume, *Polymers* **2020**, *12*, 209.
[50] J. A. Howarter, J. P. Youngblood, *Langmuir* **2006**, *22*, 11142.
[51] R. A. Shircliff, P. Stradins, H. Moutinho, J. Fennell, M. L. Ghirardi, S. W. Cowley, H. M. Branz, I. T. Martin, *Langmuir* **2013**, *29*, 4057.
[52] Y. Tian, H. Zhang, J. Zhao, T. Li, B. X. Bie, S. N. Luo, Z. Zhang, *Compos Part A Appl. Sci. Manuf.* **2016**, *90*, 62.
[53] Z. Zhao, J. Deng, H. Tae, M. S. Ibrahim, S. Suresh, N. J. Cho, *Adv. Mater.* **2022**, *32*, 2109367.
[54] Y. Cui, Y. J. Wang, Z. Y. Shao, A. R. Mao, W. W. Gao, H. Bai, *Adv. Mater.* **2020**, *32*, 1908249.
[55] Y. Hwang, M. S. Bin Ibrahim, J. Y. Deng, J. A. Jackman, N. J. Cho, *Adv. Funct. Mater.* **2021**, *31*, 2101091.
[56] S. S. Lam, R. K. Liew, C. K. Cheng, N. Rasit, C. K. Ooi, N. L. Ma, J. H. Ng, W. H. Lam, C. T. Chong, H. A. Chase, *J. Environ. Manage.* **2018**, *213*, 400.
[57] G. A. El-Din, A. A. Amer, G. Malsh, M. Hussein, *Alex. Eng. J.* **2018**, *57*, 2061.
[58] M. Husseien, A. A. Amer, A. El-Maghraby, N. A. Taha, *Int. J. Environ. Sci. Technol.* **2009**, *6*, 123.
[59] X. F. Sun, R. C. Sun, J. X. Sun, *Bioresource Technol.* **2004**, *95*, 343.
[60] P. Calcagnile, I. Caputo, D. Cannoletta, S. Bettini, L. Valli, C. Demitri, *Mater Design* **2017**, *134*, 374.
[61] G. Deschamps, H. Caruel, M. E. Borredon, C. Bonnin, C. Vignoles, *Environ. Sci. Technol.* **2003**, *37*, 1013.
[62] H. Guan, Z. Y. Cheng, X. Q. Wang, *ACS Nano* **2018**, *12*, 10365.
[63] F. Liu, M. L. Ma, D. L. Zang, Z. X. Gao, C. Y. Wang, *Carbohydr. Polym.* **2014**, *103*, 480.
[64] T. F. Fan, S. Park, Q. Shi, X. Y. Zhang, Q. M. Liu, Y. Song, H. Chin, M. S. Bin Ibrahim, N. Mokrzecka, Y. Yang, H. Li, J. H. Song, S. Suresh, N. J. Cho, *Nat. Commun.* **2020**, *11*, 1449.

